7.14   **THE DEVELOPMENT OF STANDARDIZED ANOMALIES FOR GRADIENT FIELDS AS WELL AS OTHER FIELDS - A PRELIMINARY INVESTIGATION**

1. INTRODUCTION

Most meteorological events have traditionally been diagnosed and post-analysis performed using the actual value of the parameter chosen [for example, Lifted Index (LI) or Total Totals (TT)]. As of late, standardized anomalies (Grumm and Hart, 2001) have begun to gain wider usage. This is partly due to the fact that standardized anomaly methods are an attempt to not only determine how large a parameter is, but also determine how much of a "departure from normal" the parameter is. Most applications of standardized anomalies have been to non-gradient fields such as the heights of constant pressure surfaces, mean sea level pressure, temperature, and precipitable water. Vertical gradient fields have been explored (while looking at vertical wind shear in order to form a graphic), but little, if any, application has been made to gradient fields in the horizontal.

There are some excellent candidates for the application of standardized anomaly methods in order to examine gradient fields. In the western states surface pressure gradient fields are frequently used to diagnose and predict the character of the coastal marine layer, the associated low clouds and its effect on temperatures.   For example, onshore pressure gradient flow (higher pressure west of the coastline and lower pressure east of the coastline) typically results in stronger winds, an increase in low cloudiness, and cooler conditions in comparison to "weak flow" (surface pressure east of the coastline nearly the same as that west of the coastline). Even the trend of the surface pressure gradient (usually the 24 hour change in the pressure gradient) is important. This is especially important for the development of a Catalina Eddy (Rosenthal, 1972). An offshore pressure gradient trend to the northeast along with an onshore pressure gradient trend to the east is a prime setup for the development of a

*Corresponding author address: Ivory J. Small, NOAA/NWS San Diego. 11440 W. Bernardo Ct., Ste. 230, San Diego, CA 92127-1643; e-mail; ivory.small@noaa.gov

Catalina Eddy circulation. These eddies can rapidly increase the low clouds and the amount of cool air moving inland while the coastal marine layer deepens. This flow can lift any easterly flow off the surface, generate areas of strong wind shear, and may adversely affect air travel in and out of southern California (Figure 1).

Aloft, height gradient fields are useful for looking at the possibility of stalled baroclinic zones over southern California, notorious for producing long episodes of heavy rainfall with flooding. In these cases the baroclinic zone moves very slowly and can produce training echoes and very heavy, continuous rainfall. Just the residence time of the cold, unstable airmass increases the likelihood of flooding and/or severe weather. Height gradients can also be used to help determine the strength of wind events (including Santa Ana Winds). This information is important for looking at coastal wind damage from onshore flow events as well as fire potential and wind damage during offshore flow events, (especially in the fall when fuels are still dry and Santa Ana wind frequency is on the rise). Strong winds also affect air travel, ground travel, and create property damage due to blowing dust, downed trees and power lines. Strong cross winds can develop at major airports and on major highways. The winds can cause aborted landings and can blow over trucks.

In this paper, examples will be used to illustrate the utility of standardized anomalies for looking at gradient fields and indices. Short term climatological approximations (datasets of less than 10 years of data) will be used to estimate the means and standardized anomalies. The first example to be presented is a severe weather case. During this storm a comma cloud moved onshore over the southern California Bight region, resulting in mini-supercell thunderstorm activity.   Large hail, microbursts, waterspouts and tornadoes dotted the region, not unlike the type of scenario seen in other parts of the country (except with more localized effects, as is typical for this area). The second case is a "low level blocking ridge" case where the pre-

frontal 850 mb ridging slows down the initial front, allowing a secondary front to nearly catch up, resulting in a longer period of heavy rain (over 6 inches in 6 hours at one site). The third case is an offshore flow case where wind gusts reached 90 mph in highly populated areas. These cases should give a good overview of the utility of standardized anomalies calculated from horizontal gradient fields.

2. THE 19 FEBRUARY 2005 FALLBROOK-RAINBOW-TEMECULA MINI SUPERCELL TORNADO

The strong Pacific storm of 19 February 2005 was a good example of severe weather associated with rather shallow mini-supercells in southern California, (relatively common with the stronger Pacific storms during the late fall through early spring). Analysis of cool season severe weather events have been performed in the past in southern California. Halvorson (1971) looked at a southern California severe weather outbreak characterized by cold air funnels and tornadoes. Hales (1986) brought a different approach to the problem and discussed the role of the blocking coastal terrain on the vertical wind shear profile (helicity). Blier and Batten (1994) studied the climatology of California tornadoes. Small et al. (2002) looked at a handful of cool season severe weather events, which included waterspouts, a microburst, a large hail case, and even a tornado that formed on a cloud line extending downwind from one of the offshore islands. It was seen that thunderstorms containing long lived, well defined couplets (base velocity or storm relative velocity) were good candidates for severe weather and should be watched. The storm featured in the following section displays many of the characteristics of such storms.

Figure 2 is the 06 hour forecast of the 1200 UTC 19 February 2005 NAM80 500 mb heights and 850 mb winds valid at 1800 UTC 19 February 2005. Overlaid is the 1600 UTC surface observation data and the 1530 UTC visible satellite imagery. Conditions are similar to those seen in Hales (1985). The center of the upper level low is off the central California coast. The main frontal system is in Arizona during the time of the severe weather. The comma cloud that produces the severe weather is moving through the southern

California coastal waters and onto the mainland. The comma cloud was over the Southern California Bight Region (essentially the area from the coastal slopes of the higher mountains westward). There is a trailing cold front associated with the comma. Since the comma was over the basin without a well developed cold front, there was a strong possibility that the locations of the very heavy rainfall and severe weather would be very variable. (When comma heads are further north, severe weather conditions more closely resemble a squall line rather than very isolated cells. This is because the tail supplies a more isolated lifting mechanism as it moves through, rather than the broad dynamics found closer to the comma head).

Figure 3 is the 00 hour forecast of the 1200 UTC 19 February 2005 NAM80 500 mb heights, vorticity, and 850 mb winds valid at 1200 UTC 19 February 2005. Overlaid is the 1500 UTC surface observation data and the 1430 UTC infrared satellite imagery. The comma cloud is shown moving into the coastal areas. The 500 mb heights and vorticity shows a 16 s^{-1} vorticity center producing a negative tilt diffluent trough in cold, unstable post frontal flow driving right into the coastal areas. The difluence can be seen in the 500 mb height contours. A wave of this magnitude (vorticity center of 16 s^{-1}) is rather tame in comparison to most fronts. Vorticity centers associated with stronger frontal systems are more on the order of 25-40 s^{-1}. What is different during events like the 19 February 2005 event is the cold, conditionally unstable airmass from the initial frontal passage is still over the area during these follow-on waves, as opposed to the airmasses comprised of mainly "potential instability" ahead of the "large initial frontal passages". This is one of the reasons why thunder generally occurs after a frontal passage rather than with the frontal passage in southern California. In the cold airmass behind the initial frontal band it does not take much for the event to "go severe". Conditions on 19 February 2005 were made more volatile because of the negative tilt, diffluent nature of the wave. It can be seen that this wave is not far behind the initial front. These "follow on" waves have the tendency to produce severe weather in southern California, and if the waves are even closer together, an extended period of rainfall can ensue. A well defined comma cloud is noted in the infrared satellite

Fig. 1. Terrain map of the WFO SGX CWFA. Color coding in the legend is in thousands of feet MSL. The sounding sites are indicated in red.
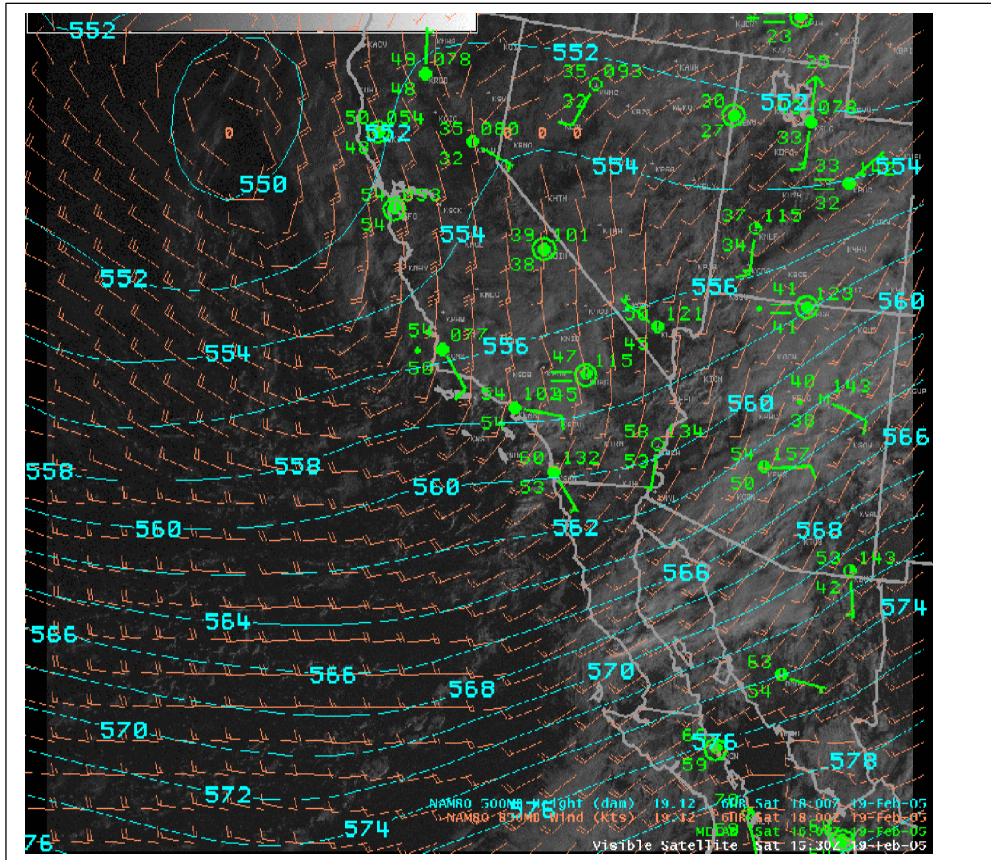
Fig. 2. The 06 hour forecast of the 1200 UTC 19 February 2005 NAM80 500 mb heights (cyan, dashed, in decameters) and the 850 mb wind barbs (orange) valid at 1800 UTC. Overlaid is the 1600 UTC surface METAR observation data (green) and the 1530 UTC visible satellite imagery. The center of the upper level low was off the central California coast. Of particular interest is the surface winds in the Southern California Bight Region are perpendicular to the 850 mb winds for increased vertical shear in the boundary layer, resulting in enhanced helicity.
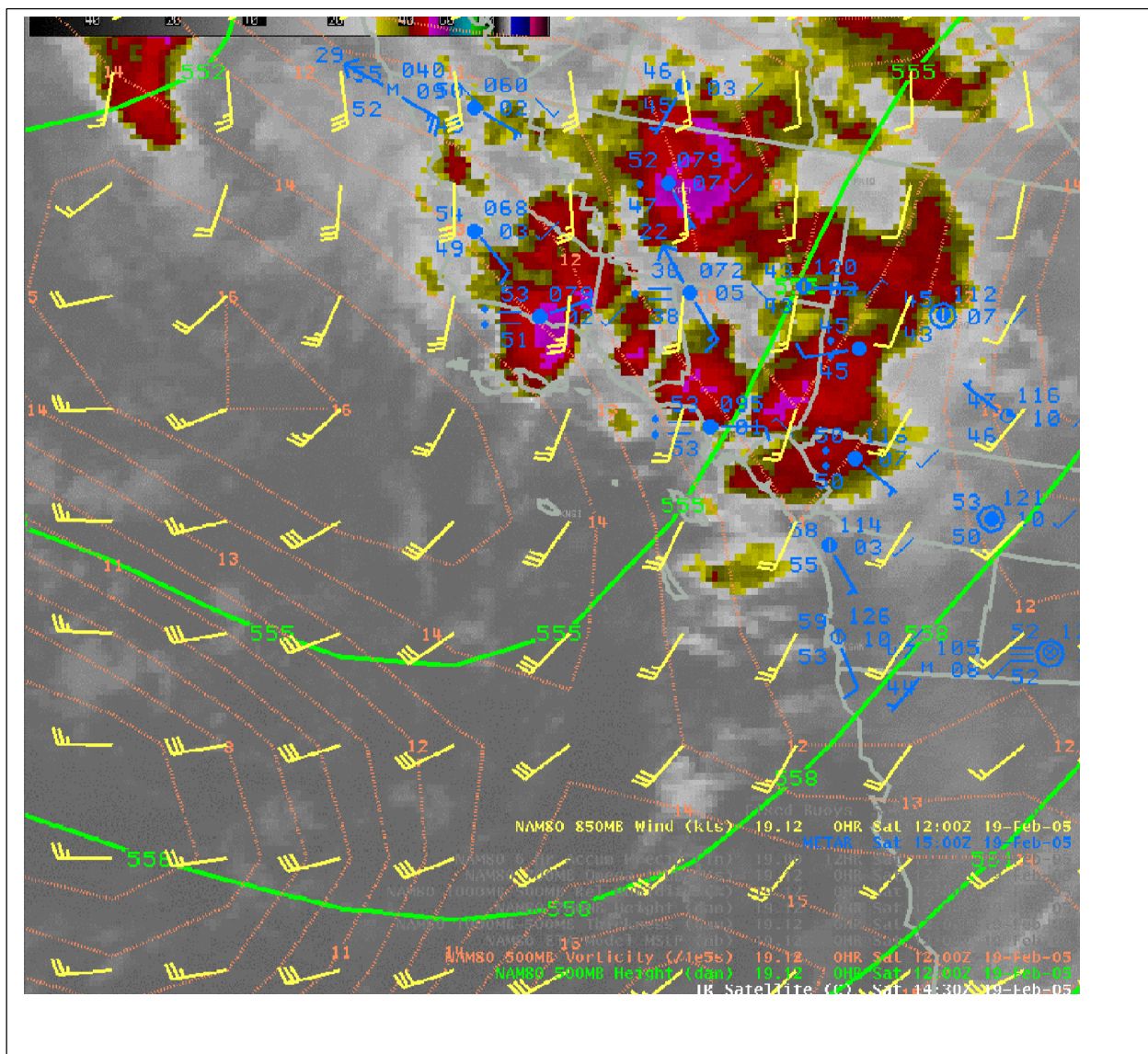
Fig. 3. The 1430 UTC 19 February 2005 infrared satellite imagery overlaid by the NAM80 00 hour 500 mb heights (green, solid, in decameters) and vorticity (orange, dotted, s^{-1}) along with the 850 mb winds (yellow, barbs) valid at 1200 UTC 19 February 2006. Also overlaid is the 1500 UTC surface METAR observation data (cyan). Notice the negative tilt trough approaching the coast associated with a vorticity maximum along with an obvious comma cloud.
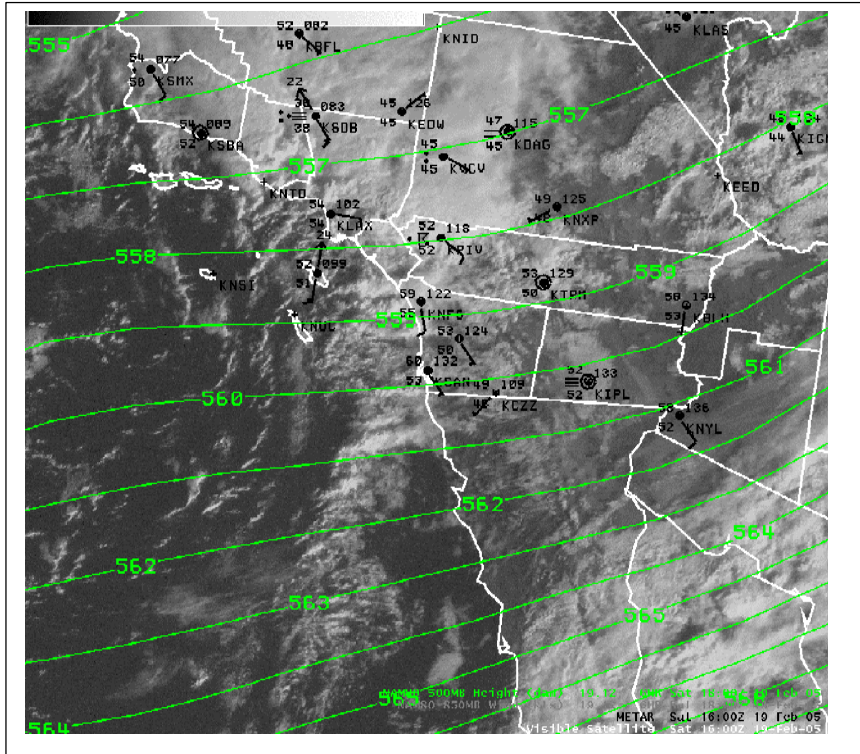
Fig. 4. Shown is the 1200 UTC 19 February 2005 NAM80 forecasted 500 mb heights (green, solid, in decameters) valid at 1800 UTC 19 February 2005 overlaid by the 1600 UTC 19 February 2005 visible satellite imagery and the 1600 UTC surface METAR observation data (black). There is severe convection along the tail of the comma cloud, with cirrus blowing off the tops of the larger (likely supercellular) thunderstorms.

Fig. 5. The 1200 UTC 19 February 2005 Miramar (KNKX) sounding shows a surface parcel with a very low LCL, and the sounding is conditionally unstable throughout much of the troposphere. Note the veering wind profile with about 20 knots (10 ms^{-1}) of 850 mb southerly flow.
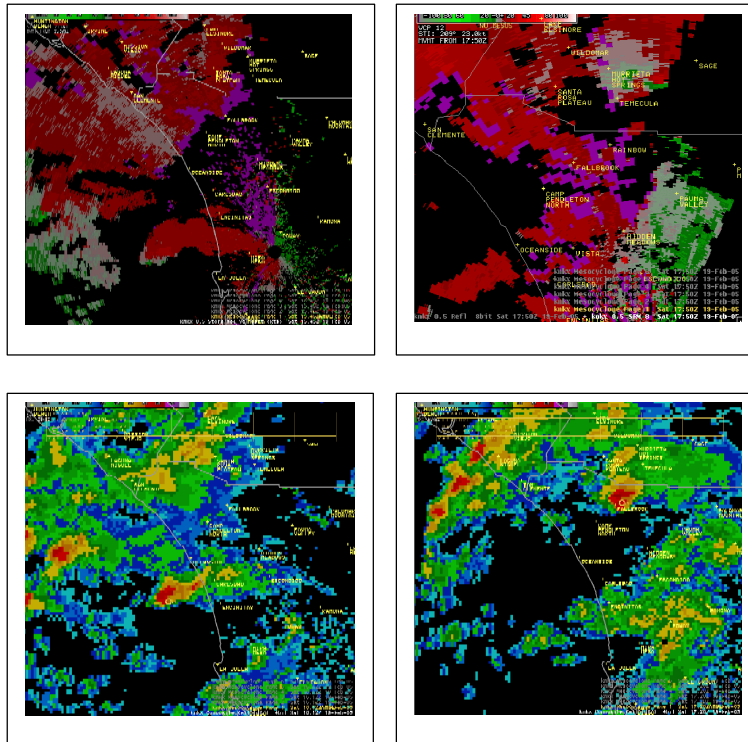
Fig. 6. The upper left panel is the 1545 UTC 19 February 2005 0.5 degree storm relative velocity. The tornadic cell that struck Fallbrook can be seen as a small inbound/outbound couplet just west of La Jolla. The upper right panel is the 1750 UTC 19 February 2005 0.5 degree storm relative velocity showing the cell exiting Temecula some 2 hours later. The couplet associated with the storm was generally steady state, and long lived since it remained intact for over 2 hours. The lower left panel is the 1612 UTC 19 February 2005 composite reflectivity, which shows this supercell just west of Oceanside. The lower right panel, the 1720 UTC 19 February 2005 KNKX composite reflectivity, shows the cell over Fallbrook at the time of the first tornado report. Although the storm was rather small, the mesocyclone detection algorithm indicated a mesocyclone associated with the storm (denoted by the yellow ring near the updraft region of the storm). There is a rather obvious "hook" visible at 1720 UTC, around the beginning of the tornadic phase of the storm.
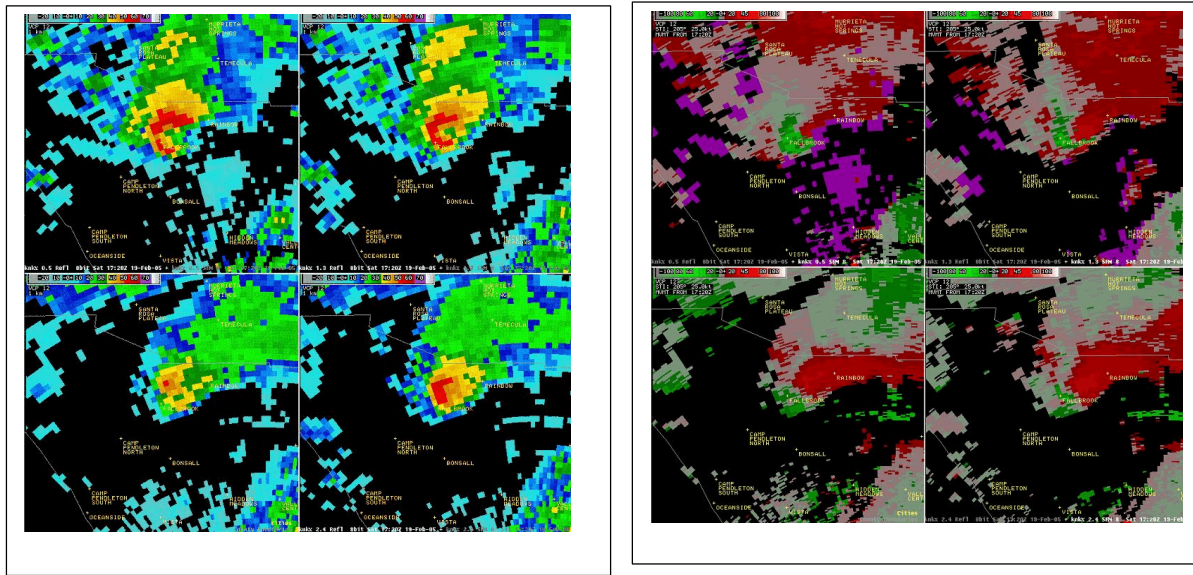
Fig. 7. On the left is the 1720 UTC 19 February 2005 KNKX radar base reflectivity (R) 4-panel at 0.5, 1.3, 2.4, and 3.1 degrees respectively. On the right is the 1720 UTC 19 February 2005 KNKX radar storm relative velocity (SRM) 4-panel at 0.5, 1.3, 2.4, and 3.1 degrees respectively. The tornadic activity developed at about 1717 UTC and lasted until about 1743 UTC. Notice the flanking line and the bounded weak echo region. With inbound velocity values of 24 knots and outbound values of 21 knots (gate to gate), the difference is around 45 knots. This is rather large, (and likely to have a high potential for tornadic activity since it exceeds 30) for southern California, but probably rather weak for much of the rest of the nation.
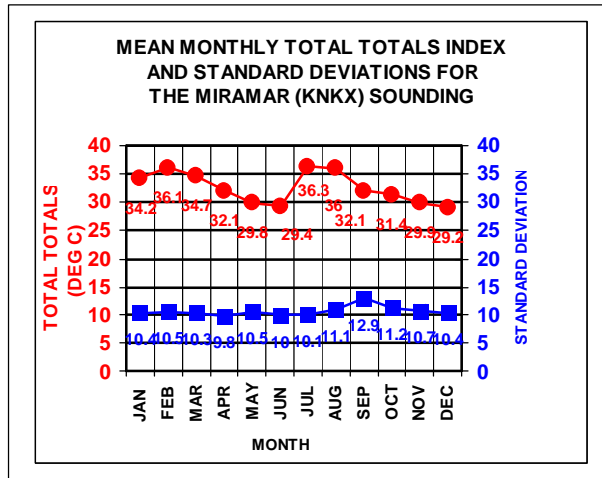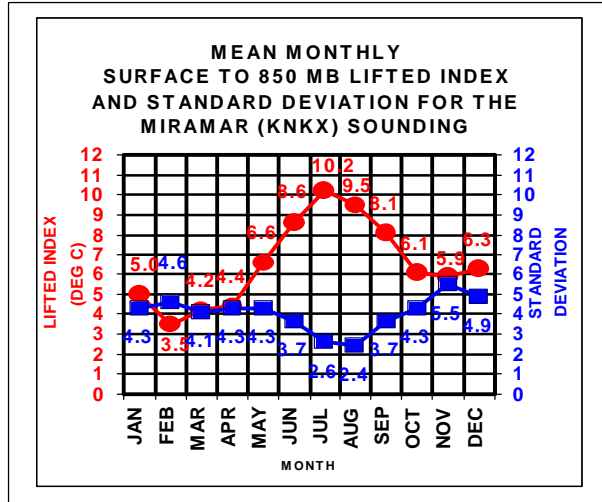
Fig. 8. The upper panel is the average surface to 850 mb lifted index for the period 1998-2005 (red, circles) along with the standard deviation (blue, squares) for the Miramar (KNKX) sounding. There is an annual minimum in the atmospheric stability in February along with a local maximum in the standard deviation in February as well These are probably due to the big variations cause by the big storms of February. There is a peak in the lifted index during mid summer since the summer subsidence inversion is based below 850 mb. Since summer is a rather stable time of the year for the boundary layer at KNKX, the standard deviation reaches the annual minimum. There were a total of 5768 soundings out of a possible 5844 soundings available. The lower panel is the mean monthly total totals index (red, circles) along with the standard deviation for the period 1998-2005 for the Miramar (KNKX) sounding (blue, squares). There seems to be a bi-modal aspect to the total totals index (instability), with a maxima during the strong storms of the " rainy season" (February peak) and during the " monsoon season" (July peak). There are minima during the late spring " stratus season" (June minimum) and the mid to late fall during the heart of the "Santa Ana Season" (December minimum). There seems to be a possible standard deviation peak in September, probably due, in part, to the fight between the more stable Pacific airmass and the unstable airmasses of the monsoonal and tropical storm airmasses. In summary, there is a peak in instability for both indices in February. There is a peak in the instability aloft in the summer, but the boundary layer is stabilized by the marine layer inversion. There were a total of 5701 soundings out of a possible 5844 soundings available.

imagery of this case. There is a very "cellular" characteristic to the activity in the comma head, and it is also apparent along the tail of the comma cloud. Figure 4 is the 1200 UTC 19 February 2005 NAM80 forecasted 500 mb heights valid at 1800 UTC overlaid by the 1600 UTC 19 February 2005 visible satellite imagery and the 1600 UTC surface METAR observation data. There is severe convection along the tail of the comma cloud, with cirrus blowing off the tops of the larger (likely supercellular) thunderstorms. Figure 5 is the 1200 UTC 19 February 2005 Miramar (KNKX) sounding. It shows a surface parcel with a very low LCL, and the sounding is conditionally unstable throughout much of the troposphere. Note the veering wind profile with about 20 knots (10 ms^{-1}) of 850 mb southerly flow. The event shows a surface based moist layer with a conditionally unstable lapse rate. The first report of severe weather was associated with the head of the comma in the Orange County area (in the vicinity of KSNA). [The further from the low center a location is, the colder the temperatures aloft need to be for thunderstorms to develop. For example, weak upper level lows with rather high temperatures at 500 mb (warmer than -20 C) can produce thunderstorms if it is overhead, but if it is displaced somewhat to the north, the -20 degree contour is usually needed for thunderstorms to occur. In this case the 500 mb temperatures were well under -20 C (actually down around -25 C)]. As for severe weather, a 3/4 inch diameter hail report was received at 1452 UTC. Later a waterspout moved onshore as a tornado with damage in Huntington Beach, near KSNA, at 1542 UTC 19 February 2005. A mini-supercell thunderstorm resulted in tornado reports from Fallbrook to Temecula between 1717 UTC and 1743 UTC 19 February 2005. A microburst produced gusts to 70 knots in Laguna Hills, about 6 miles inland in Orange County at 1815 UTC 19 February 2005.

In Figure 6 the upper left panel is the 1545 UTC 19 February 2005 0.5 degree storm relative velocity. The tornadic cell that struck Fallbrook can be seen as a small inbound/outbound couplet just west of La Jolla. The upper right panel is the 1750 UTC 19 February 2005 0.5 degree storm relative velocity showing the couplet and associated

cell exiting Temecula some 2 hours later. The couplet associated with the storm was generally steady state, and long lived, remaining intact for over 2 hours. The lower left panel is the 1612 UTC 19 February 2005 composite reflectivity, which shows this supercell just west of Oceanside. The lower right panel, the 1720 UTC 19 February 2005 KNKX composite reflectivity, shows the cell over Fallbrook, where the first tornado report was from. Although the storm was rather small, the mesocyclone detection algorithm indicated a mesocyclone associated with the storm (denoted by the yellow ring in the updraft region of the storm). There is a rather obvious "hook" visible at 1720 UTC, around the beginning time of the tornadic phase of the storm.

Figure 7 shows the 4-panel KNKX radar data for the Fallbrook-Rainbow-Temecula mini-supercell. The tornadic activity developed at about 1717 UTC and lasted until about 1743 UTC. Notice the flanking line and the bounded weak echo region. With inbound velocity values of 24 knots and outbound values of 21 knots (gate to gate), the shear was around 45 knots. This is apparently enough for tornado development in southern California, but probably much less than optimal for tornado development in most areas of the country.

Standardized anomalies were created for this event. In figure 8 the upper panel is the average surface to 850 mb lifted index for the period 1998-2005 along with the standard deviation for the Miramar (KNKX) sounding. There is an annual minimum in the atmospheric stability in February along with a local maximum in the standard deviation in February as well The large variations in February are probably caused by the big storms of February. There is a peak in the lifted index during mid summer since the summer subsidence inversion is based below 850 mb. Since this is a rather stable pattern, the standard deviation reaches the annual minimum. (There was a total of 5768 soundings out of a possible 5844 soundings available). The lower panel in figure 8 is the mean monthly total totals index along with the standard deviation for the period 1998-2005 for the Miramar (KNKX) sounding. There

seems to be a bi-modal aspect to the total totals index (instability), with a maxima during the strong storms of the "rainy season" (February peak) and during the "monsoon season" (July peak). There are minima during the late spring "stratus season" (June minimum) and the mid to late fall during the heart of the "Santa Ana Season" (December minimum). There seems to be a possible peak in September, probably due, in part, to the fight between the more stable Pacific airmass and the unstable monsoonal and tropical storm airmasses. In summary, there is a peak in instability for both indices in February. There is a peak in the instability aloft in the summer, but the boundary layer is stabilized by the marine layer inversion. (There was a total of 5701 soundings out of a possible 5844 soundings available).   Figure 9 shows the actual values for the 19 February 2005 case. The upper panel is the total totals index along with the 850 mb wind speed in knots and the 850 mb wind speed in m s^{-1}. The lower panel is the standardized anomaly of the total totals index and the standardized anomaly of the surface-to-850 mb lifted index. The total totals values reached approximately 56 during this event, which is a standardized anomaly of about 1.9. The surface to 850 mb lifted index fell to -2.47, which is a standardized anomaly of -1.3. This shows that surface to 850 mb lifted indices approaching -2 (standardized anomaly values around 1) and total totals above about 50 (standardized anomalies of over 1) during the cool season can result in severe, even supercellular convection in southern California. Typically without the strong upper level support seen with this case, it is more likely that waterspouts and funnel clouds would be the main result.

3. THE 20 OCTOBER 2004 HEAVY RAINFALL CASE.

An early season Pacific storm produced 11.24 inches of rainfall in the mountains of southern California at Lytle Creek, with 6.22 inches falling in only 6 hours, and 10.02 inches in 24 hours. The height gradients were well above normal during this storm. Figure 10 shows the mean monthly 850 mb height gradient between the Miramar (KNKX) and Tucson (KTUS) soundings. Also shown are the standard deviation of the height gradient and the standard deviation of the trend (the trend being the 24 hour change in the height

gradient) for the period 1998-2002 at 1200 UTC.   The height gradient is negative in December and January, indicating higher heights at Miramar than at Tucson during those months. The height gradient is more or less steady during the summer, but falls to become negative in December and January. The largest standard deviations appear to be mid/late winter (February) with the lowest values mid summer. It also seems that the height gradients are inversely proportional to the standard deviation. (There were 1717 of a possible 1826 1200 UTC soundings available).

The left panel of figure 11 is the 2315 UTC 19 October 2004 infrared satellite imagery. It shows a very strong cold front catching up to a previous cold front. The cold front produced 6 inches of rainfall in 6 hours and nearly a foot of rainfall for the storm total. The right panel is the 1800 UTC 20 October 2004 0000 hour GFS40 850 mb heights and winds. There is a very strong low level jet over San Diego. Figure 12 shows the Miramar (KNKX) to Tucson (KTUS) 850 mb height gradient along with its standardized anomaly. Notice the whopping standardized anomaly of 4.3, indicating how unusual such a strong height gradient is for October.   The low level jet at 850 mb reached 34 knots (around 18 ms^{-1}), and along with 1000-500 mb mean relative humidity in excess of 80 percent the storm was a prime candidate for flash flooding.

Bimonthly values of MEI (the Multivariate ENSO Index) consisting of pairs such as (January/February and February/March) are called bimonthly seasons (NOAA, 2006). They have been computed beginning with the December 1949/January 1950 season to the present. A value of 1 would denote the strongest La Nina case for that bimonthly season, while the highest number (56 or 57) would indicate the strongest El Nino case. For instance, for the December-January bimonthly "season" the strongest La Nina was recorded in 1974 (an MEI of 1), while the strongest El Nino occurred in 1983 (an MEI if 57). Terciles (or "thirds") are also used to split up the values into ranges in order to define the event magnitude. For instance 1-19, 20-37, and 38-57 defines a weak to strong La Nina, near neutral, and weak to strong El Nino conditions respectively. Figure 13 contains the MEI values for the heart of the winter rainy season (January/February) for the years 1998-2002.

TOTAL TOTALS INDEX ALONG WITH 850 MB WIND SPEED

STANDARDIZED ANOMALY OF THE TOTAL TOTALS INDEX ALONG WITH THE SURFACE TO 850 MB LIFTED INDEX AND ITS STANDARDIZED ANOMALY AT MIRAMAR (KNKX)
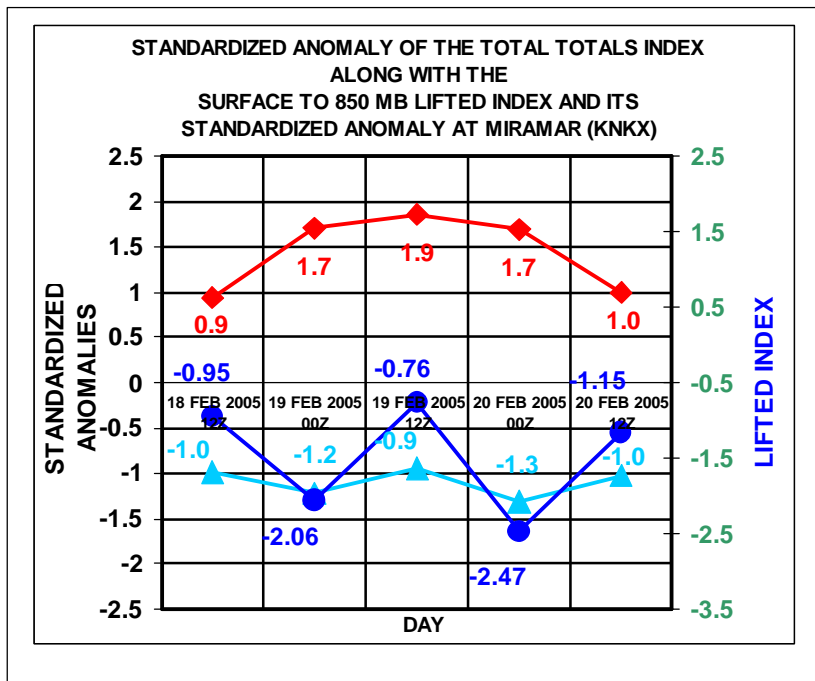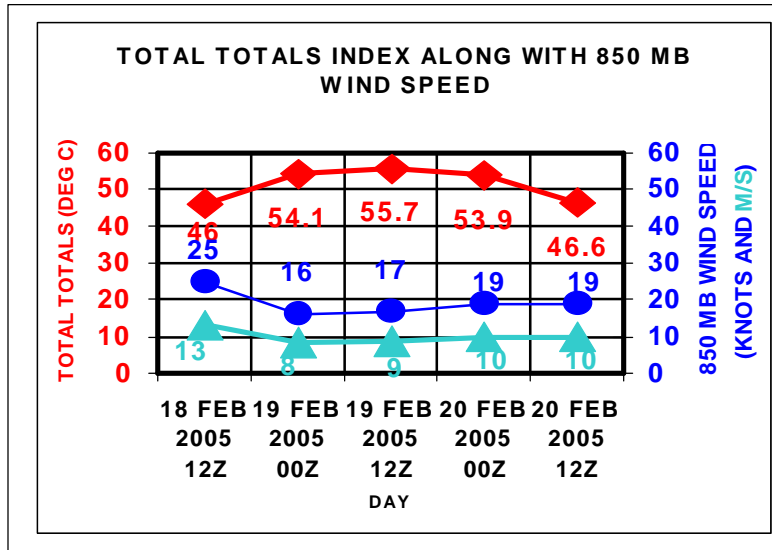
Fig. 9. The upper panel is the total totals index (the highest curve, red, diamonds) along with the 850 mb wind speed (middle curve, blue, circles), and the 850 mb wind speed in ms^{-1} (the lowest curve, cyan, triangles). The lower panel is the standardized anomaly of the total totals index (the upper curve, red, diamonds, the surface to 850 mb lifted index (dark blue, circles), and the standardized anomaly of the surface to 850 mb lifted index (cyan, triangles).
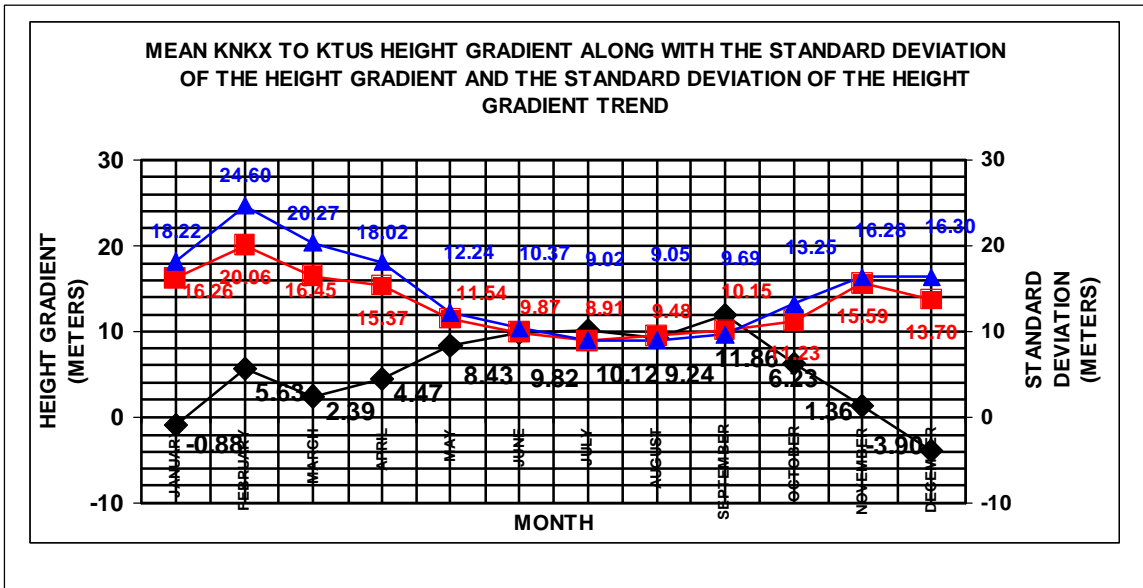
Fig. 10. Graphic shows the mean monthly 850 mb height gradient between the Miramar (KNKX) and Tucson (KTUS) soundings (black, diamonds). Also shown are the standard deviation of the height gradient and the standard deviation of the trend (the trend being the 24 hour change in the height gradient) for the period 1998-2002 at 1200 UTC. The height gradient is negative in December and January, indicating higher heights at Miramar than at Tucson during those months. The height gradient is more or less steady during the summer, but falls to become negative in December and January. The largest standard deviations are during the mid/late winter (February), likely due to the very strong storms (possibly the strongest of the year) during that time period. There may also be a local maximum in the height gradient in February. The lowest values are during mid summer. It appears that the height gradients are inversely proportional to the standard deviations. There were 1717 of a possible 1826 1200 UTC soundings available.
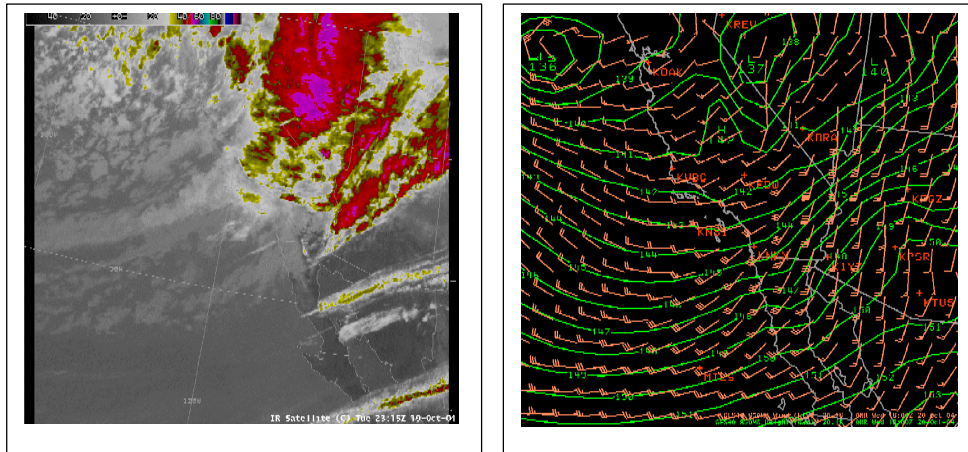
Fig. 11. The left panel is the 2315 UTC 19 October 2004 infrared satellite imagery showing the very strong frontal system that produced over 6 inches of rainfall in 6 hours and nearly a foot of rainfall for the storm total. The right panel is the 00 hour 850 mb heights (green, solid) along with the 850 mb wind barbs (knots) valid at 1800 UTC 20 October 2004.
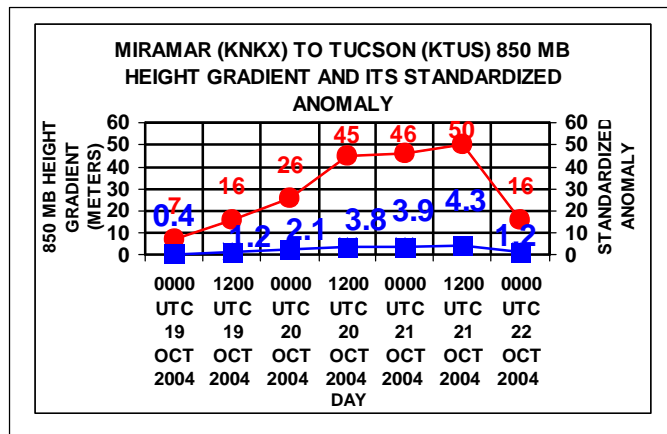

Fig. 12. The figure is a comparison of the KNKX to KTUS sounding 850 mb height gradient (red, circles) and its standardized anomaly (blue, squares) during a major Pacific storm. Large positive values indicate that the movement of the storm system from west to east is hampered. Especially notable is the standardized anomaly value of 4.3. This value indicates a huge blocking ridge to slow down the cold front, create a strong southerly subtropical flow, and is a good sign that very heavy rainfall with flooding is possible.
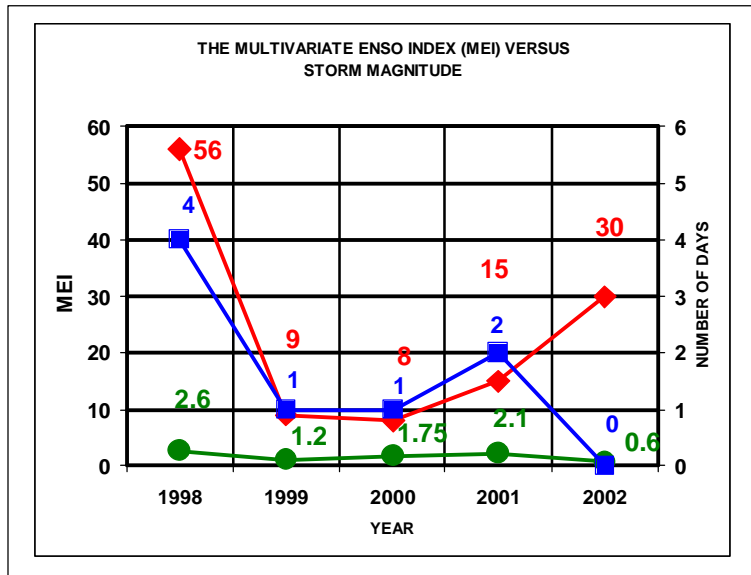
Fig. 13. The figure is a graph of the Multivariate ENSO Index (MEI) for February of 1998, 1999, 2000, 2001, 2002 (the red curve with the diamonds), the number of soundings with a peak KNKX to KTUS 850 MB height gradient of 60 meters or more (blue with squares), and the average of the 5 highest February standard anomalies (green, circles) for each year. There was a peak in the number of soundings with large blocking during the strong El Nino of 1998, with a significant drop during the years of 1999-2001 when the MEI was also low. There were 263 of a possible 281 soundings available.

COMPARISON OF THE LSF-RIC SURFACE PRESSURE GRADIENT AND STANDARD DEVIATION FOR THE SURFACE PRESSURE GRADIENT AND THE SURFACE PRESSURE GRADIENT TREND
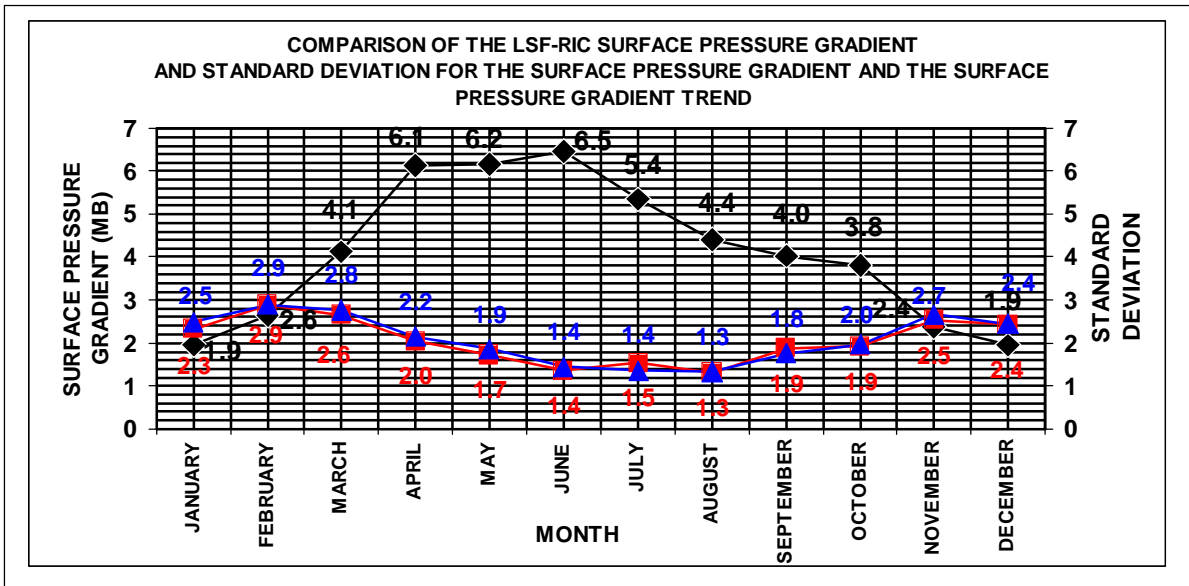
Fig.14. This figure shows the annual cycle of the Las Flores (LSF) to Rice Valley (RIC) surface pressure gradient taken at 1200 UTC for the years 2000-2003. The 1200 UTC soundings were used to eliminate the diurnal aspects of the surface pressure gradient, which typically decreases overnight to a minimum near sunrise, and increases during the day to a maximum near sunset. It can be seen that the variations are so large in the winter that the standard deviation is larger than the actual surface pressure gradient. The local maximum in the surface pressure gradient in February may be a reflection of the large Pacific storms. The local maximum in the standard deviation in November may be a reflection of the increasing episodes of offshore flow events. During the quieter summer period, the surface pressure gradient can be 4 times the size of the standard deviation. Also note that the standard deviation of the surface pressure gradient is nearly equivalent to the size of the standard deviation of the 24 hour surface pressure gradient trend. There were 1019 of a possible 1461 soundings available.
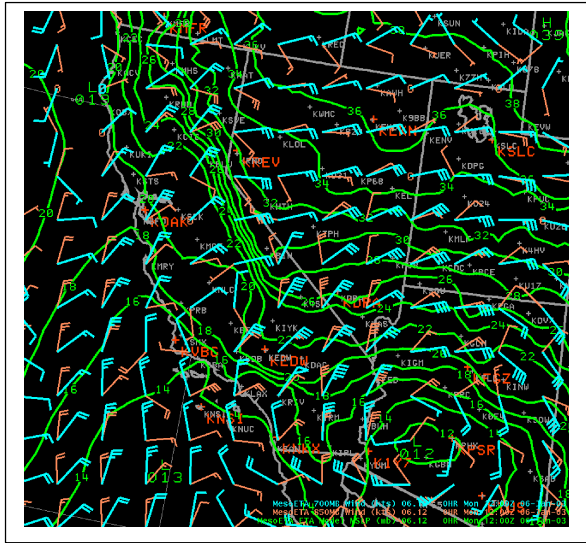

Fig. 15. The above figure is the 1200 UTC 6 January 2003 mean sea level pressure (green, solid, in mb) overlaid by the 850 mb winds (orange, knots) and the 700 mb winds (cyan, knots).

1200 UTC LAS FLORES TO RICE VALLEY SURFACE PRESSURE GRADIENT AND STANDARDIZED ANOMALY
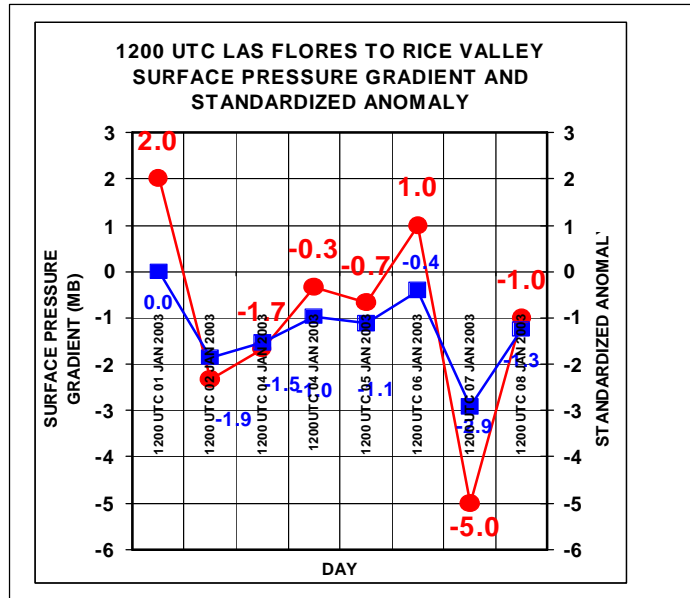
Fig.16. The graphic is the comparison between the 1200 UTC surface pressure gradient (in mb) between Las Flores (LSF) and Rice Valley (RIC) between 1 January 2003 and 8 January 2003 and the standardized anomaly. The pressure gradient is the red curve with the circles. The standardized anomaly is the blue curve with the squares. At the time of the minimum in the surface pressure gradient (-5.0 mb) there was also a rather respectable minimum in the standardized anomaly (-2.9) in this case. The 24 hour pressure gradient trend for the time period ending at 1200 UTC 7 January 2003 was a whopping -6.0 mb.
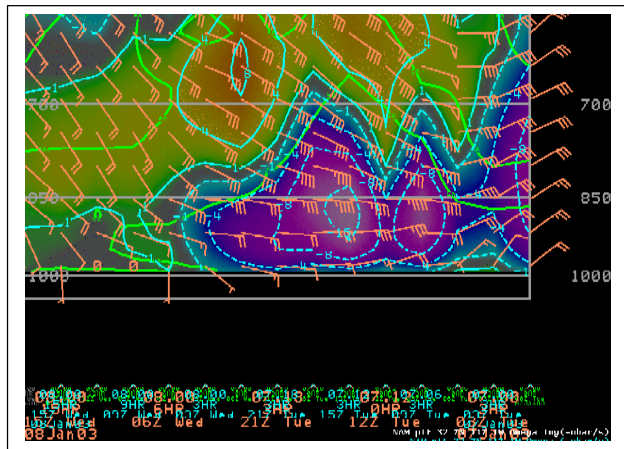
Fig.17. NAM40 1200 UTC time/height crossection of the winds (knots) and omega (cyan contours and shading, microbars/sec) at San Diego (KNKX). The time begins at 0000 UTC 7 January 2003 on the right and increases from right to left. There is the typical veering of the winds with time from northeast to southeast, which results in strong winds in the north-south passes at the beginning of an event, then strong winds in the east-west passes toward the end of an event. (The wind veers with time at the surface to possibly form an eddy at the end). If the upper level low and post frontal surface high develops too far to the east, no significant winds develop, and there is only warming. At other times the lows cut off and strengthen to the southeast of the region, with strongest winds in the southern portion of the forecast area (rather than the usual scenario when strongest winds are in the northern portion of the forecast area).

The values, which consist of 56, 9, 8, 15, and 30 indicates that for the 5 year period, conditions in 1998 began as a strong El Nino, fell immediately to a weak La Nina in 1999, then finally increase to become a "near neutral" pattern by 2002. A strikingly similar pattern was noted in the number of storms which contained 850 mb blocking of 60 or higher. The strong low latitude jets of an El Nino year may cut down on the number of strong offshore flow events, but increase the number of (and wind damage near the coast associated with) the strong Pacific storms and their onshore flow type winds.

4. THE 6-7 JANUARY 2003 STRONG SANTA ANA WIND CASE

Figure 14 shows the annual cycle of the Las Flores (LSF) to Rice Valley (RIC) surface pressure gradient taken at 1200 UTC for the years 2000-2003. (The 1200 UTC soundings were used to eliminate the diurnal aspects of the surface pressure gradient, which typical decreasing overnight to a minimum near sunrise, and increases during the day to a maximum near sunset). It can be seen that the variations are so large in the winter that the standard deviation is larger than the actual surface pressure gradient. During the quieter summer period, the surface pressure gradient can be 4 times the size of the standard deviation. Also note that the standard deviation of the surface pressure gradient is nearly equivalent to the size of the standard deviation of the 24 hour surface pressure gradient trend. (There were 1019 of a possible 1461 soundings available).

On 6-7 January 2003 a deep upper level low pressure system resulted in strong pressure gradients over the southwestern states (figure 15) along with large standardized anomaly values. In combination with strong upper level flow from the northeast and a tight cold air gradient aloft (with the cold air to the northeast), widespread winds in excess of 50 knots (26 ms^{-1}) developed. A wind gust at Ontario International Airport (KONT) reached 78 knots (40 ms^{-1}), which is 90 mph. Figure 16 shows a comparison between the 1200 UTC surface pressure gradient (in mb) between Las Flores (LSF) and Rice Valley (RIC) between 1 January 2003 and 8 January 2003 and the standardized anomaly. At the time of the minimum in the surface pressure gradient (-5.0 mb) there was also a rather respectable minimum in the standardized anomaly (-2.9) in this case. The 24 hour pressure gradient trend for the time period ending at 1200 UTC 7 January 2003 was a whopping -6.0 mb. Figure 17 is the NAM40 forecast time/height cross section of the winds and omega at San Diego (KSAN). The time begins at 0000 UTC 7 January 2003 on the right and increases from right to left. There is the typical veering of the winds with time from northeast to southeast, which results in strong winds in the north-south passes at the beginning of an event, shifting to strong winds in the east-west passes toward the end of an event. (The wind veers with time at the surface. This could form a Catalina Eddy which can make forecast high temperatures too high near the end of the event). Forecasting these events can be tricky. If the upper level low develops too far east, no significant winds develop, and there is only warming. At other times if the low cuts off and strengthens to the southeast or south of the forecast area, the strongest winds are more likely to be in the southern portion of the forecast area (rather than in the northern part of the forecast area seen during a typical event).

5. DISCUSSION AND CONCLUSION

It has been seen that standardized anomalies add valuable information to the analysis and forecast process. For winter severe weather, it seemed that standard anomalies of only 1 to 2 for the total totals index and the surface-to-850 mb lifted index were sufficient for the production of severe weather for southern California on 19 February 2005. The total totals index showed an annual cycle, with a peak in February associated with the strong storms of winter, and another peak in July associated with the North American Monsoon. The surface to 850 mb lifted index showed a minimum (most unstable) value in February, also likely to be due to the large storms in February. The 850 mb height gradient between KNKX and KTUS showed a positive value in the summer (higher 850 mb heights at KTUS than at KNKX) which likely reflects the monsoonal high, and shows a minimum in December, interestingly, near the peak of the "offshore flow season" in southern California. The size of the positive height gradients is correlated with storms that produce very

heavy rain. And finally, the Multivariate ENSO Index (MEI) for February of 1998-2002 (although a very small sample) showed some correlation between the number of soundings with large positive heights gradients (hence standardized anomalies) between KNKX and KTUS and whether or not the MEI indicated an El Nino or La Nino year. Thus standardized anomalies for both horizontal gradient fields as well as for indices have been shown to be a very useful tool for the researcher as well as the forecaster.

6. REFERENCES

Blier, W. and K. A. Batten, 1994: On incidence of tornadoes in California. *Wea. Forecasting,* **9**, 301-315.

Grumm, R. H. and R. E. Hart, 2001: Standardized Anomalies Applied to Significant Cold Season Weather Events: Preliminary Findings. *Weather and Forecasting,* **16**, 736-754.

Hales, J. E., Jr., 1985: Synoptic features associated with Los Angeles tornado occurrences. *Bull. Amer. Meteor. Soc.*, **66**, 657-662

Halvorson, D. A., 1971 Tornado and Funnel Clouds in San Diego County. Western Region Technical Attachment No. 71-33. Available from NWS Western Region, P. O. Pox 11188, Salt Lake City, UT 84147

Hart, R., and R. H, Grumm, 2000: Using normalized climatological anomalies to rank synoptic scale events objectively. *Mon. Wea. Rev.,* **129**, 2426-2442.

Small, I., G. Martin, S. LaDochy, and J. Brown, 2002: Topographic and Synoptic Influences on Cold Season Severe Weather Events in California. Preprints of the 16th Conference on Probability and Statistics, Orlando, FL, Amer. Meteor Soc., 146-153. http://ams.confex.com/ams/pdfpapers/28708.pdf

National Oceanic and Atmospheric Administration, Earth System Research Laboratory, Physical Science Division (2006); http://www.cdc.noaa.gov/people/klaus.wolter/MEI/rank.html

Rosenthal, J., 1972: Point Mugu Forecasters Handbook. Pacific Missile Range Tech. Publ. PMR-TP-72-1. 278 pp. [Available from Pacific Missile Range, Pt. Mugu, CA 93042-5000.]